J Mol Model (2014) 20:2167
DOI 10.1007/s00894-014-2167-y

ORIGINAL PAPER

A combined experimental and computational study of the esterification reaction of glycerol with acetic acid

Gabriel Alejandro Bedogni · Cristina Liliana Padró · Nora Beatriz Okulik

Received: 9 December 2013 / Accepted: 4 February 2014

Abstract This work describes theoretical and experimental studies on glycerol esterification to obtain acetins focusing on the obtained isomers. The reaction of glycerol with acetic acid was carried out on Amberlyst 36 wet. Density functional theory calculations on the level of M06-2X functional and 6-311+G(d,p) basis set are carried out and the most stable structures of the reactants and products are located by considering a large number of conformers. The thermodynamics is discussed in terms of the calculated reaction Gibbs free energy. The AIM theory was used to characterize reactants and products. The glycerol esterification with acetic acid is found to be thermodynamically favored, with exothermal property. These agree well with experiments and allow us to explain the relative selectivity of products.

Keywords AIM analysis · Catalysis · Density functional theory · Glycerol esterification

Introduction

The manufacture of first generation biodiesels (fatty acid alkylesters) by transesterification processes has been growing continuously during the last years, mainly due to the renewable source of this fuel in comparison with the conventional fuels derived from petroleum [1, 2]. Consequently a large amount of glycerol is produced (accounts for 10 wt% of the total product) which has to be revaluated in order to make the bio-fuel industry economically and environmentally viable [3].

As a matter of fact, the market for glycerol is now saturated and the production of valuable chemicals such as fuel and raw molecules for polymer industry from this compound, seems to be a promising solution leading to an increase in market novel opportunities. Within the studies of glycerol utilization pathways, it is worth to mention some research directed toward reactions forming molecules which improve the quality of biodiesel by reducing the viscosity and cloud point or by decreasing the particulate emission. In this sense, it could be mentioned that the products issued from the etherification of glycerol with tert-butanol and isobutylene can be used as additives in biodiesel [4–6]. Glycerol can also react with aldehydes, ketones, acetic acid and methyl, ethyl acetates forming acetals, cetals, and glycerine acetates that can be used for reducing the particulate emission and for improving combustion and the biodiesel behavior at low temperature [7–10].

In particular, the esterification of glycerol into acetins is quite attractive due to the versatile industrial application of the final products, going from cosmetic to fuel additives [11].

The products of glycerol esterification with acetic acid are: monoacetins, MAG: 1-monoacetin, 1-MAG and 2-monoacetin, 2-MAG, diacetins, DAG: 1,2-diacetin,1,2-DAG and 1,3-diacetin, 1,3-DAG and triacetin, TAG, (Scheme 1). Monoacetin can be used as a food additive, in the manufacturing of explosives and smokeless powder and mixed with diacetin and triacetin for printing inks, plasticizers and softening agents [12].

In addition, MAG and DAG could be used as solvent, plasticizer, softening agent and solvent for dyes, while the mixture of MAG and DAG has applications in chemical

Electronic supplementary material The online version of this article (doi:10.1007/s00894-014-2167-y) contains supplementary material, which is available to authorized users.

G. A. Bedogni · N. B. Okulik (✉)
Departamento de Ciencias Básicas y Aplicadas, Universidad Nacional del Chaco Austral, Cdte. Fernández 755, Pcia, 3700 Roque Sáenz Peña, Chaco, Argentina
e-mail: nora@uncaus.edu.ar

C. L. Padró
Grupo de Investigación en Ciencias e Ingeniería Catalíticas (GICIC), INCAPE (UNL- CONICET), Santiago del Estero 2654, 3000, Santa Fe, Argentina

Published online: 16 March 2014

Scheme 1 Products of glycerol esterification

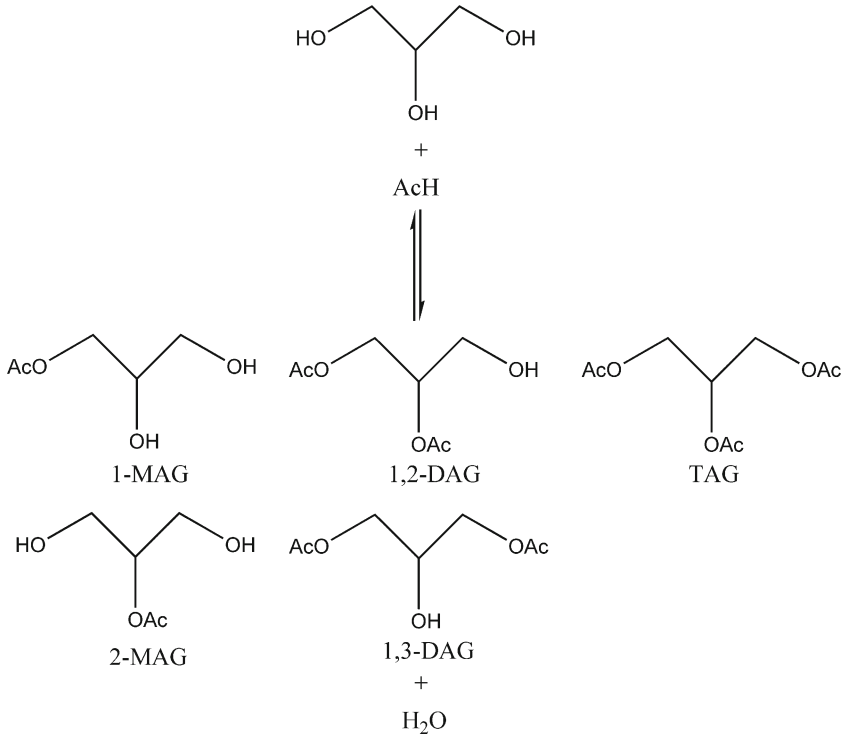

products in food [13]. TAG is the most useful acetin, being used as a food additive, plasticizer, antifungal agent, and additive for gasoline [6]. Further details about several new ways to valorize glycerol can be found in [11, 14–19] and references therein.

Among all the existing possibilities to strike glycerol overproduction, we focus our investigation on the esterification of glycerol with acetic acid in order to form species which could be used as bio-fuels additives or raw materials for the production of biodegradable polyesters [2, 20], mainly MAG, DAG, and TAG.

Several type of catalysts [2, 21–27] have been used for the acetylation of glycerol. Gonçalves et al. [20] compared the different performances of catalysts, including ion exchange resins, which showed the best catalytic activity. Good selectivity of diacetin was achieved over zeolite supported dodecamolybdophosphoric [25, 27, 28]. The influence of reaction conditions on product distribution in the heterogeneous acetylation of glycerol with acetic acid was determined over Amberlyst 15 [29]. The parameters of the acetylation of glycerol reaction were optimized on different solid acid catalysts by Zhou et al. [30].

Even though there are a considerable number of papers that deal with this topic, very few of them focus on the theoretical study of esterification of glycerol reaction. Liao et al. have carried out theoretical calculations on glycerol esterification reactions locating the most stable structures of all acetylated glycerol derivates which are in agreement with the corresponding experimental results [31]. The thermodynamics was discussed in terms of the calculated reaction Gibbs free energy. The glycerol esterification with acetic acid was found to be thermodynamically unfavourable, while its esterification with acetic anhydride was favored with a significantly exothermal property. Jamroz et al. have done simulation work on the etherification of glycerol and they have found that the substitution of glycerol is preferred at the terminal positions rather than at the central C–O group [32].

Despite the large number of experimental works that have been reported, only a few papers distinguish the two kinds of monoacetins (1-MAG and 2-MAG) and diacetins (1,3-DAG and 1,2-DAG) [20, 21]. Consequently, an experimental and theoretical study about the esterification of glycerol with acetic acid, with the aim of addressing this issue can be very useful to explain the relative occurrence of the formed species.

The motivation of the current study is to characterize, on theoretical grounds, the experimental results of the glycerol esterification with acetic acid reaction focusing on the obtained isomers. For that purpose, we have carried out detailed theoretical calculations to provide some valuable fundamental insights on transformation of glycerol into acetins. The nature of the interactions between chemical reagents is better understood by carrying out calculations on reaction Gibbs free energy and by topological analysis of electronic structure.

Experimental

Preliminary experiments were carried out in order to establish the influence of the most significant reaction variables on the glycerol conversion and selectivity on Amberlyst 36 wet. Variables included in the study (optimization study) were

agitation, the acetic acid to glycerol molar ratio, and temperature. The optimum reaction conditions were: agitation = 800 rpm, T=413 K, acetic acid:glycerol = 6 mol:1 mol.

The liquid phase glycerol esterification with acetic acid was carried out in a stainless steel batch reactor (Parr 4560). The reactor was loaded with glycerol and pretreated commercial resin Amberlyst 36 Wet (mass ratio of catalyst/glycerol = 5 wt%). The temperature in the reactor was raised up to 413 K and the necessary amount of acetic acid to reach 6:1 acetic acid:glycerol molar ratio was incorporated. The mixture was heated to the reaction temperature (413 K) and maintained constant for 4 h (total reaction time). The reactor pressure was kept at 405.3 kPa by using N_2 as inert gas. The reaction mixture was continuously stirred.

The products were analyzed by GC on a Agillent Technologies 6850 gas chromatograph equipped with a 30 m Innowax column (inner diameter: 0.32 mm, film thickness: 0.5 mm) and a flame ionization detector (FID).

The AIM theory

The atoms-in-molecules (AIM) theory [33–35] reveals insightful information on the nature of bonds. This theory is based on the critical points (CP) of the electronic density, $\rho(\mathbf{r})$. These are points where the gradient of the electronic density, $\nabla\rho(\mathbf{r})$, vanishes and are characterized by the three eigenvalues (λ_1, λ_2, λ_3) of the Hessian matrix of $\rho(\mathbf{r})$. The CPs are labeled as (r, s) according to their rank, r (number of nonzero eigenvalues), and signature, s (the algebraic sum of the signs of the eigenvalues).

Four types of CPs are of interest in molecules: (3, −3), (3, −1), (3, +1), and (3, +3). A (3, −3) point corresponds to a maximum in $\rho(\mathbf{r})$ and it appears generally at the nuclear positions. A (3, +3) point indicates electronic charge depletion and is known as cage critical point; (3, +1) points, or ring critical points, are merely saddle points. Finally, a (3, −1) point, or bond critical point, is generally found between two neighboring nuclei indicating the existence of a bond between them.

Several properties that can be evaluated at the bond critical point, BCP, constitute very powerful tools to classify the interactions between two fragments. The two negative eigenvalues of the Hessian matrix (λ_1 and λ_2) at the BCP measure the degree of contraction of $\rho(\mathbf{r})$ perpendicular to the bond toward the critical point, while the positive eigenvalue (λ_3) measures the degree of contraction parallel to the bond and from the BCP toward each of the neighboring nuclei. Unequal values of λ_1 and λ_2 at (3, −1) BCP's denote an anisotropic spread of electrons quantified through the concept of ellipticity: $\varepsilon = \lambda_1/\lambda_2 - 1$, (with $\lambda_1 > \lambda_2$) where values of $\varepsilon >> 1$ can be indicative of π bonding. Calculated properties at the BCP of the electronic density are labeled with the subscript 'b' throughout the work.

In the AIM theory atomic interactions are classified according to two limiting behaviors, namely, shared interactions (large values of ρ_b and $\nabla^2\rho_b<0$), characteristic of covalent and polarized bonds, and closed-shell interactions (small values of ρ_b and $\nabla^2\rho_b>0$), useful to describe ionic bonds, hydrogen bonds, and van der Waals interactions.

AIM theory permits the identification of reactive sites by means of the Laplacian of the charge density, $\nabla^2\rho$. AIM defines the valence-shell charge concentration (VSCC) as the outer molecular zone where $\nabla^2\rho<0$. This zone is the one which, upon chemical combination, is distorted to yield non-bonded critical points (NBCP), which are minima in $\nabla^2\rho$ (maxima of charge concentration), corresponding in number and position to the electron pairs defined by the Lewis and related models [33]. NBCP correspond to zones where an electrophilic attack can occur.

Computational methods

The compounds studied are very flexible. Indeed, glycerol itself has been reported to have at least 100 conformers [36]. However, a search of conformers of each of the studied molecules would exceed the scope of this paper and therefore we performed some kind of qualitative calculations. The conformational space of the reactants and products was investigated using molecular dynamics simulations as implemented in the HyperChem package [37]. The semiempirical AM1 method was used as the force field [38].

The molecules were heated from 0 to 800 K in 0.1 ps. The system temperature was then kept constant by coupling the system to a thermal bath with a bath relaxation time of 0.5 ps [39]. After an equilibration period of 5 ps, simulation was accomplished saving the molecular cartesian coordinates every 5 ps. The time step for all the simulations was 1.0 fs.

The resulting geometries were then optimized using AM1 with a threshold of 0.1 kcal $Å^{-1}$ mol^{-1} in the RMS gradient. Such simulations and geometry optimizations were carried out with the Hyper-Chem package.

The AM1-optimized geometries of the lowest-energy conformers obtained according to the above methodology were further optimized using tools from density functional theory [40–42] as implemented in the Gaussian 09 package [43]. These calculations were accomplished using the Beck three-parameters hybrid exchange-correlation functional, known as B3LYP [44–46], and the hybrid functional M06-2X of Truhlar and Zhao [44, 47]. The 6-311+G(d,p) basis set is used for all atoms. The local minima on the potential energy hypersurface were characterized by the computation of the vibrational frequencies at the same level of theory used in the geometry optimizations. The absence of vibrational modes with

imaginary frequencies shows that the optimized molecular geometries are at a local minimum in the potential energy hypersurface.

Only those optimized geometries lying up to 2 kcal mol^{-1} above the lowest-energy conformer of every molecule were considered for further studies. The energy threshold of 2 kcal mol^{-1} provides some confidence that the contribution of higher energy conformations is less than 8 % to every property measured at 413 K, according to the Maxwell-Boltzmann distribution.

In order to facilitate the comparison of theoretical results with experimental data, further geometry optimizations and calculation of properties were performed including solvent (acetic acid) effects through the polarizable continuum model [48–50] as implemented in the Gaussian 09 package.

The thermochemistry data were evaluated at experimental temperature and pressure conditions (413 K and 405.3 kPa). Gibbs free energies (from vibrational harmonic normal-mode computations) were calculated at M06-2X/6-311+G(d,p) level using Gaussian 09 package [43]. All correction factors and frequencies are not scaled.

Topological charge density was displayed by the AIM method [33] using the program AIMAll [51]. Wave functions (as the only input information required for the topological analysis) were calculated at M06-2X/6-311++G(d,p) level.

Results and discussions

Experimental results

Table 1 shows results of glycerol esterification with acetic acid experimentally measured in this study. In the conditions that the reaction was performed, glycerol was almost completely transformed into the products (the glycerol conversion after 4 h of reaction was 93 %) with 1-MAG and 1,3-DAG as the main products of reaction.

It can be seen that the amount of 1-monoacetin is about 18 times the amount of 2-monoacetin, while 1,3-DAG concentration is twice the 1,2-DAG concentration. The concentration of TAG reached 0.174 $mol.l^{-1}$ (7.8 % of the total product concentration).

Table 1 Product distribution of the glycerol esterification with acetic acid over Amberlyst 36[a]

Product	Concentration (mol l^{-1})
1-MAG	0.901
2-MAG	0.048
1,2-DAG	0.365
1,3-DAG	0.738
TAG	0.174

[a] Reaction conditions: temperature = 413 K, pressure = 405.3 kPa, acetic acid:glycerol = 6 :1, *t*=4 h, catalyst = Amberlyst 36 Wet (mass ratio catalyst/glycerol = 5 wt%)

Conformational search and geometry optimization

The methodology described above leads to several different conformations in the gas phase of glycerol and its acetylated derivatives. In general we found two or three structures near in energy while the remaining conformations are found to be higher in energy than the threshold of 2 kcal mol^{-1} and they were not considered for further analysis. Except for glycerol, for which we have carried out an extensive analysis on its structures, we selected a unique structure for each studied compound.

The atom numbering of the studied structures are shown in Fig. 1.

Glycerol structures

The conformation of glycerol has been extensively studied in the gas [36, 52], liquid [53, 54], and solid states (X-ray analysis) [55] and the conformational space of the molecule is quite complex.

Geometries and vibrational frequencies of the stationary points were first optimized at the B3LYP/6-311+G(d,p) level, and then M06-2X/6-311+G(d,p) calculations were conducted. In the present work, we considered three glycerol structures (conformers **1**, **2** and **3**) whose conformations have lower energy than the threshold of 2 kcal mol^{-1} with respect to the most stable one in the gas phase. The relative energies and some selected structural parameters of the conformers **1**, **2** and **3** are listed in Table 2. Moreover, the geometric parameters when the solvent effect was used are also shown for conformer 1. The results of two related works [31, 56] are also listed in Table 2 together with experimental results [55].

As we have mentioned, glycerol is a very flexible molecule so the structures **1**, **2**, and **3** differ substantially only in their dihedral angles. Then, we used the most stable structure, **1**, for further comparisons.

The bond lengths of glycerol evaluated in the present work with B3LYP and M06-2X methods are in good agreement with those of previously reported theoretical results using B3LYP calculations [31, 56] (Table 2).

Generally, it is expected that the bond lenghts calculated by electron correlated methods are slightly longer than the experimental values and the bond and dihedral angles are slightly different because the molecular states differ during experimental and theoretical processes. One isolated molecule is considered in gas phase during theoretical calculation, while many packing molecules are treated in condensed phase during the experimental measurement. This situation can be observed in Table 2, as expected, bond lengths yielded by

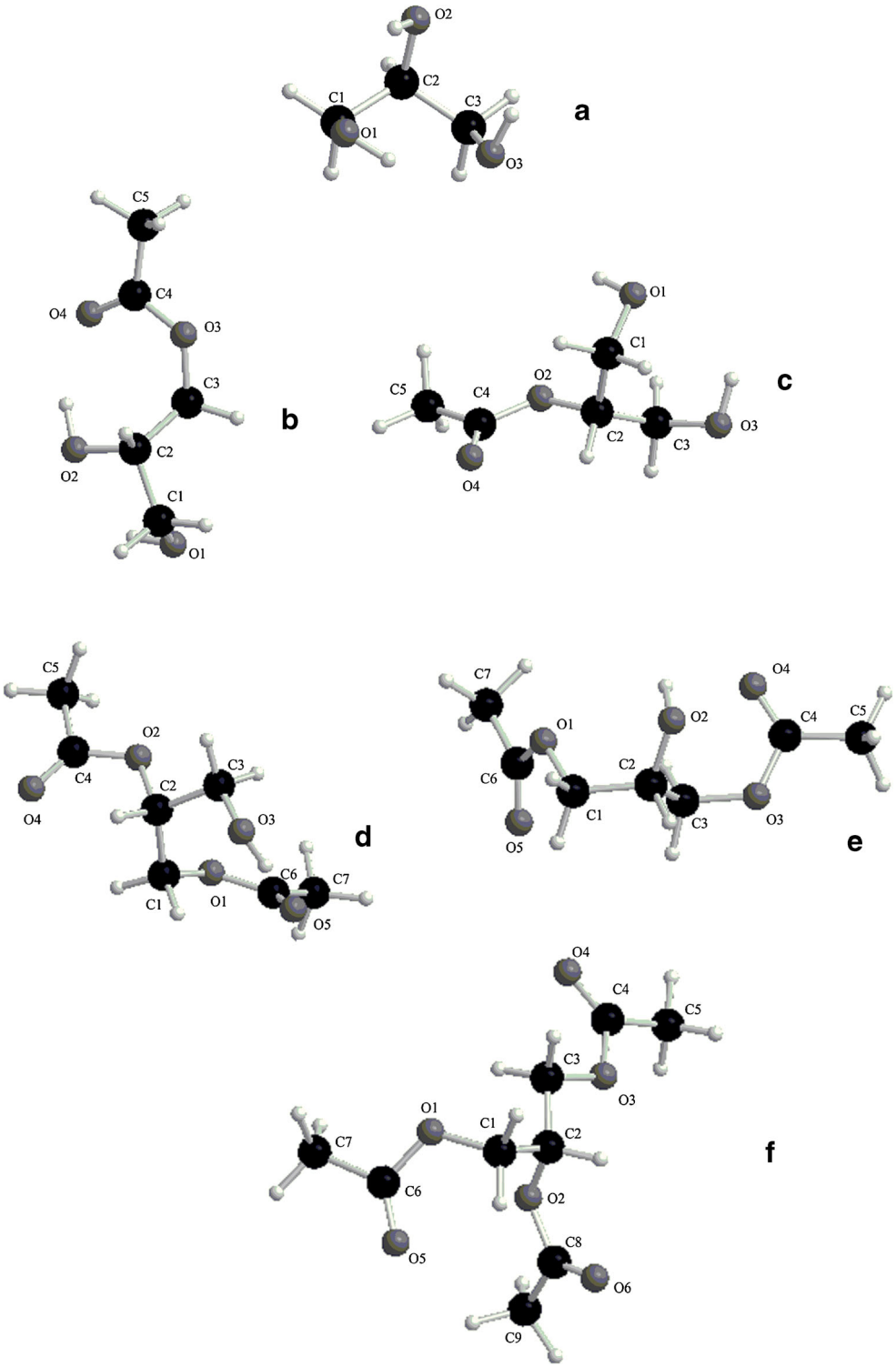

Fig. 1 Atom numbering of glycerol **a** and products of glycerol acetylation: 1-MAG (**b**), 2-MAG (**c**), 1,2-DAG (**d**), 1,3-DAG (**e**) and TAG (**f**)

B3LYP and M06-2X of our calculations are slightly overestimated in comparison with the experimental data.

The root-mean-square deviations (RMSD) between experimental [55] and our theoretical values for each method were calculated to investigate the performance of the both DFT methods in predicting the bond lengths of glycerol. RMSD between calculated bond lengths and experimental values are 0.029 Å for B3LYP, 0.025 Å for M06-2X and 0.027 Å when the solvent effect was used.

Regarding dihedral angles, the calculations at M06-2X/6-311+G(d,p) including the solvent effect level (Table 2) better predicts the values of the angles than the calculated values at

Table 2 Selected bond lengths (in angstroms) and bond and dihedral angles (in degrees) of the three stable conformers of glycerol found within 2 kcal mol^{-1} with respect to the most stable one[a,b]

Connected atoms	1 [c]	1 [d]	2 [d]	3 [e]	From ref. [56]	From ref. [31]	Exp.[e]
ΔE (kcal mol^{-1})	0.00 (0.00)	0.00 (0.00)	0.47	1.14			
E_{total} (kJ mol^{-1})	−904402.463 (−904453.562)	−904434.552 (−904472.501)	−904432,602	−904429,758			
C1-C2	1.530 (1.527)	1.524 (1.521)	1.519	1.521	1.524	1.531	1.509
C1-O1	1.434 (1.439)	1.423 (1.427)	1.423	1.410	1.430	1.434	1.401
C1-C2-C3	113.1 (113.5)	112.6 (112.9)	112.3	112.5	112.6	112.8	–
O1-C1-C2-O2	64.0 (67.8)	−48.2 (−51.6)	−54.9	52.4	−176.4	−58.0	−59.57
O2-C2-C3-O3	−49.6 (−54.2)	61.5 (65.7)	−57.5	58.1	57.5	48.0	66.56

[a] Comparison with theoretical and experimental data is also provided. Total and relative energies are also shown. Results obtained when solvent effects are included are shown in parenthesis

[b] For atom numbering, see Fig. 1

[c] Calculated at B3LYP/6-311+G(d,p) level

[d] Calculated at M062X/6-311+G(d,p) level

[e] Taken from ref. [55]

B3LYP/6311+G(d,p) level. For example, the calculated O2-C2-C3-O3 dihedral angle has opposite sign at B3LYP/6311+G(d,p) level.

Therefore, we concluded that the M06-2X method leads to a better prediction of the structures of the studied compounds when the solvent effect is considered.

It is very interesting to note that, although it has little impact on the gas-phase geometries, the inclusion of solvent effects better predicts the dihedral angles. Moreover, the use of solvent effect makes a more realistic description of catalytic phenomenon, then we decided to perform all our calculations at M06-2X/6-311+G(d,p) level.

Glycerol acetylated derivatives structures

Upon the results obtained on glycerol structures, we concluded that the calculated geometric parameters represent good approximations and they can be used as the foundation to calculate the rest of the studied compounds. Consequently, the B3LYP-optimized geometries of the lowest-energy conformers of glycerol acetylated derivatives obtained according to the adopted methodology were further optimized using M06-2X functional. Then we have chosen one conformer of each molecule which was energetically the most stable at the M06-2X level and performed for it M06-2X/6-311+G(d,p) optimizations and the harmonic frequency calculations including solvent effects.

The calculated bond lengths and bond angles of lowest energy conformers that we have found for monoacetylglycerol, diacetylglycerol, and triacetylglycerol are shown in Tables 3, 4, and 5, respectively.

The calculated bond lengths of 1-MAG (see Table 3) fit very well with those obtained by Limpanuparb et al. [56] at B3LYP/6-31++G(d,p) level of theory and by Liao et al. [31] at B3LYP/6-31G** level of theory with a bond length RMSD of 0.028 Å and 0.032 Å, respectively, when the C1-C2-C3 atoms are superimposed. However, it should be noticed that the most stable conformers of 1-MAG reported in this work exhibited very different dihedral angles with respect to the structure reported by Liao et al. [31], probably because the σ bond permits the atoms to rotate freely in relation to each other almost without energy barrier. Similar observations can be made when comparing the calculated 2-MAG structures (Table 3) with reported values [31, 56] (bond length RMSD of 0.003 Å and 0.019 Å).

The calculated bond lengths of 1,2-DAG and 1,3-DAG (see Table 4) are similar to those obtained by Limpanuparb et al. [56] and by Liao et al. [31] with a bond length RMSD (C1-C2-C3 atoms superimposed) of 0.020 Å and 0.013 Å, respectively, for 1,2-DAG and 0.01 Å and 0.039 Å, respectively, for 1,3-DAG. Again, the most stable conformers of diacetylglycerol reported in this work exhibited different dihedral angles with respect to the similar structure reported previously [31, 56].

The same trends described above are observed in the analysis of TAG structures, similar bond lengths (bond length RMSD (C1-C2-C3 atoms superimposed) of 0.009 Å and 0.038 Å, respectively) but different dihedral angles compared with previously reported values [31, 56].

AIM analysis

It is well known that electronic characteristics are essential to reveal the nature of bonded interactions. As an advanced method that can offer a simple, rigorous, and elegant way of partitioning any system into its atomic fragments, considering the gradient vector field of its electron density, Bader's atoms

Table 3 Selected bond lengths (in angstroms) and bond and dihedral angles (in degrees) of the more stable conformer of monoacetylglycerol[a,b]

Connected atoms	1-MAG			2-MAG		
	This work [c]	From ref. [56]	From ref. [31]	This work [c]	From ref. [56]	From ref. [31]
E_{total} (kJ mol^{-1})	−1304882,178 (−1304911,820)			−1304868,204 (−1304905,405)		
C1-C2	1.521 (1.517)	1.529	1.542	1.521 (1.519)	1.529	1.531
C2-O2				1.442 (1.443)	1.457	1.444
C3-O3	1.441 (1.444)	1.442	1.450			
O3-C4	1.334 (1.332)	1.359	1.341			
O2-C4				1.350 (1.342)	1.360	1.378
C4-O4	1.208 (1.213)	1.213	1.213	1.200 (1.208)	1.212	1.200
C4-C5	1.501 (1.494)	1.507	1.502	1.503 (1.496)	1.509	1.506
C1-C2-C3	110.4 (110.6)	113.8	113.8	111.9 (113.2)	113.1	114.9
C3-O3-C4	117.5 (118.2)	116.1	118.0			
C2-O2-C4				117.1 (118.0)	61.0	131.9
O1-C1-C2-C3	−144.6 (−144.9)	−179.2	80.2	45.1 (55.8)	118.0	46.4
C2-O2-C4-C5				−177.7 (−178.8)	176.7	2.2
C3-O3-C4-C5	−175.5 (−175.3)	−179.4	177.7			

[a] Comparison with theoretical data is also provided. Total energies are also shown. Results obtained when solvent effects are included are shown in parenthesis

[b] For atom numbering, see Fig. 1

[c] Calculated at M062X/6-311+G(d,p) level

Table 4 Selected bond lengths (in angstroms) and bond and dihedral angles (in degrees) of the more stable conformer of diacetylglycerol[a,b]

Connected atoms	1,2-DAG			1,3-DAG		
	This work [c]	From ref. [56]	From ref. [31]	This work [c]	From ref. [56]	From ref. [31]
E_{total} (kJ mol^{-1})	−1705326,672 (−1705354,996)			−1705321,137 (−1705352,466)		
C1-C2	1.520 (1.518)	1.515	1.528	1.523 (1.515)	1.525	1.526
O1-C6	1.337 (1.337)	1.355	1.353	1.349 (1.343)	1.358	1.358
C6-O5	1.207 (1.212)	1.214	1.206	1.201 (1.208)	1.212	1.204
C6-C7	1.501 (1.493)	1.508	1.506	1.501 (1.495)	1.508	1.508
C2-O2	1.434 (1.438)	1.449	1.449			
C3-O3	1.404 (1.413)	1.426	1.417	1.429 (1.437)	1.449	1.445
O2-C4	1.348 (1.343)	1.359	1.361			
O3-C4				1.345 (1.339)	1.359	1.358
C4-O4	1.201 (1.208)	1.213	1.203	1.204 (1.208)	1.212	1.202
C4-C5	1.502 (1.494)	1.508	1.503	1.500 (1.495)	1.508	1.507
C1-O1-C6	118.3 (118.7)	116.2	117.9	117.6 (118.2)	116.2	117.7
C1-C2-C3	114.4 (114.7)	112.2	115.8	111.5 (111.2)	112.1	115.7
C3-O3-C4				116.7 (116.5)	116.5	115.6
C2-O2-C4	117.3 (118.1)	117.9	117.4			
O1-C1-C2-C3	−63.1 (−61.1)	70.8	−43.8	−63.8 (−177.4)	65.0	71.5
C1-C2-C3-O3	−61.5 (−62.8)	63.3	74.6			
C2-C3-O3-C4				−89.6 (−178.5)	176.7	−176.5
C2-O2-C4-C5	179.6 (179.3)	176.4	−171.5			
C3-O3-C4-C5				176.6 (179.7)	179.1	−177.6

[a] Comparison with theoretical data is also provided. Total energies are also shown. Results obtained when solvent effects are included are shown in parenthesis

[b] For atom numbering, see Fig. 1

[c] Calculated at M06-2X/6-311+G(d,p) level

Table 5 Selected bond lengths (in angstroms) and bond and dihedral angles (in degrees) of the more stable conformer of triacetylglycerol[a,b]

Connected atoms	This work[c]	From ref. [56]	From ref. [31]
E_{total} (kJ mol^{-1})	−2105764,042 (−2105793,936)		
C1-C2	1.511 (1.515)	1.528	1.527
C1-O1	1.427 (1.432)	1.441	1.435
O1-C8	1.346 (1.346)	1.360	1.363
C8-O6	1.200 (1.206)	1.212	1.202
C8-C9	1.502 (1.495)	1.507	1.503
C2-O2	1.429 (1.436)	1.447	1.446
O2-C4	1.354 (1.345)	1.362	1.363
C4-O4	1.200 (1.207)	1.212	1.202
C4-C5	1.498 (1.493)	1.507	1.511
C3-O3	1.432 (1.434)	1.442	1.427
O3-C6	1.350 (1.345)	1.356	1.355
C6-O5	1.200 (1.207)	1.214	1.206
C6-C7	1.501 (1.494)	1.508	1.506
C1-O1-C8	115.7 (118.6)	117.8	116.8
C1-C2-C3	112.0 (111.9)	112.6	115.9
C2-O2-C4	116.3 (117.1)	117.8	123.2
C3-O3-C6	117.5 (118.0	116.1	124.1
C1-O1-C8-C9	−178.0 (−177.1)	−179.1	−168.6
C2-O2-C4-C5	172.4 (176.2)	177.5	166.9
C1-C2-C3-O3	55.0 (59.3)	−171.5	−79.7
C3-O3-C6-C7	−178.7 (−177.3)	179.5	166.9

[a] Comparison with theoretical data is also provided. Total energies are also shown. Results obtained when solvent effects are included are shown in parenthesis

[b] For atom numbering, see Fig. 1

[c] Calculated at M06-2X/6-311+G(d,p) level

in molecules (AIM) theory has been applied widely to study intra and intermolecular interactions [33].

According to AIM analysis at M06-2X/6-311++G(d,p) level, the properties evaluated at the BCP corresponds to interactions attributable to covalent or polarized bonds. The values of the electron densities, ρ_b, obtained in C-C bonds are within the range of 0.2529–0.2559 a.u. and the value of $\nabla^2\rho_b$ varies from −0.6225 to −0.6059 a.u. These values reveal that there are no significant variations for these properties in each type of bond for the different structures, and these results are in agreement with results previously reported [33].

The topological properties at BCP of CO bonds showed values of an intermediate or shared polar covalent bond (high ρ_b and less than zero $\nabla^2\rho_b$ values). The topological characterization of C-O bonds from glycerol and its acetylated derivatives slightly differed from topological features of C = O bonds and it could be related to bond order. The C-O(H) bonds provide prototypes of a single bond (ρ_b~0.2490 a.u. and $-\nabla^2\rho_b$~0.3589 a.u.). Similar features show the C-O(C) bonds (ρ_b~0.2337 a.u. and $-\nabla^2\rho_b$~0.2177 a.u.) while the C = O bonds have character of a polarized double bond (ρ_b~0.4045 a.u. and $-\nabla^2\rho_b$~0.0482 a.u.).

Figure 2 shows the contour map of the Laplacian distribution, $-\nabla^2\rho$, for 1-MAG structure in the plane that contains C-C-C bonded atoms. The shared interaction between carbon atoms can be seen and the critical points at the covalent bonds C-C are located in a region of charge accumulation.

The contour map of the Laplacian distribution for 1-MAG structure in a plane that contains the ester group is displayed in Fig. 3. This pattern is slightly different from Fig. 2. It can be seen in Fig. 3 that critical points between C and O atoms are located in an area of charge depletion as anticipated by topological properties corresponding to shared polar bond.

A mechanism for the esterification reaction where the acidic groups of the catalyst initiate the reaction by donating a proton to the carboxylic acid molecule (Scheme 2) has been proposed [57, 58]. The proton attaches to the lone pair of electrons of the oxygen which is double-bonded to the carbon, and this causes the carbon to obtain a fair amount of positive charge. The carboxylic acid is accessible for a nucleophilic attack by the hydroxyl group from the alcohol and the reaction continues with water elimination. Finally, the catalyst is recovered and the ester is formed, yielding the respective mono-, di-, tri- glycerol esters.

In order to gain more insight into the site of electrophilic attack, we undertook a topological analysis of the Laplacian of the electronic density. Therefore, NBCP have been determined on the oxygen atoms bound to the H atoms in the OH groups for glycerol and 1-MAG.

Two NBCP found in the external and internal oxygen atoms are compatible with two lone electron pairs localized at the upper and lower positions of the plane, corresponding to an oxygen atom with sp3 hybridization. In glycerol, the NBCP found in the external oxygen atoms (O5 and O9) have higher values of the Laplacian of the electronic density ($\nabla^2\rho$= 5.150 a.u. and −5.120 a.u. for O9) than the NBCP found in the internal (O7) oxygen atom ($\nabla^2\rho$=−5.086 a.u. and −5.008 a.u.). Similar results were found for 1-MAG being the NBCP belonging to external oxygen atom (O5) of the Laplacian of the electronic density ($\nabla^2\rho$=−5.140 a.u. −5.127 a.u.) higher than the NBCP belonging to internal oxygen atom (O7) ($\nabla^2\rho$=−5.005 a.u. and −5.075 a.u.).

Provided that $\nabla^2\rho$ can be considered as an indicator of the electrophilic attack site, the centers with the highest $\nabla^2\rho$ value (O5 and O9 in glycerol and O5 in 1-MAG) would correspond to the preferred attack site. Then, the formation of 1-MAG from glycerol could be favored over 2-MAG. In the same direction, the 1,3-DAG formation could be favored over the 1,2-DAG formation because the external O(H) is more suitable to react with positive charged acid group, leading to the preferential formation of 1,3-DAG.

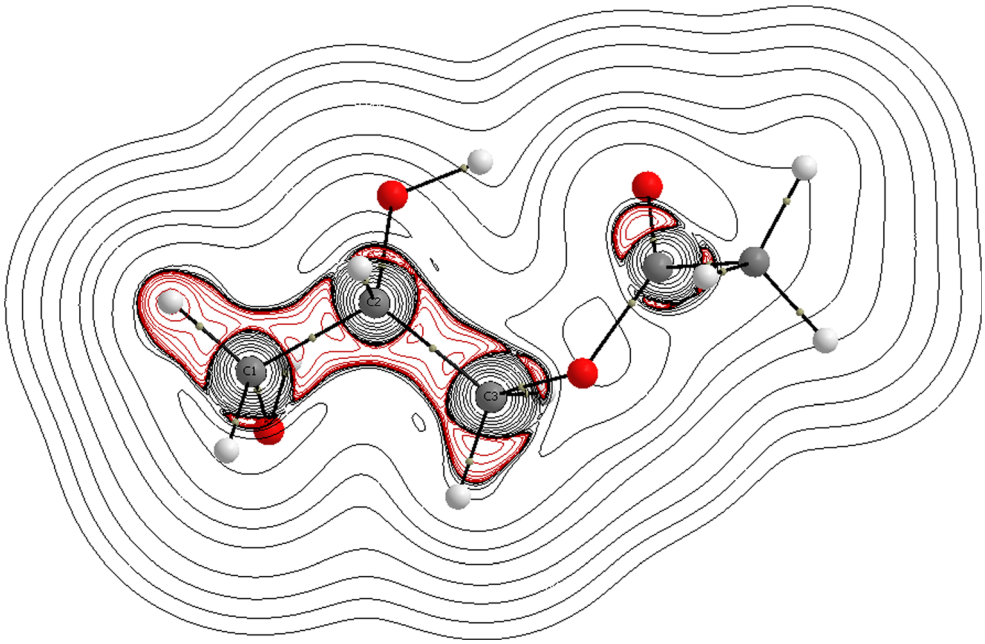

Fig. 2 Laplacian of the electronic charge density of 1-MAG in the plane that contains C-C-C bonded atoms. *Red* (broken) lines represent regions of electronic charge concentration and solid black lines denote regions of electronic charge depletion. Bond CP are indicated with *gray* circles. The molecular graph is also indicated. The contours of the Laplacian of the electronic charge density increase and decrease from a zero contour in steps of $\pm 2\times 10^n$, $\pm 4\times 10^n$, and $\pm 8\times 10^n$, with n beginning at −3 and increasing by unity

Energy analysis and mechanism of formation of TAG

The reaction is usually carried out using high acetic acid/glycerol ratio in order to push the equilibrium toward the more valuable di- and tri-acetylated products. To obtain more accurate energies the solvent effects have been considered and the energies of all structures were calculated at the M06-2X/6-311+G(d,p) level with the SCRF (PCM) method.

Gibbs free energies of reactants and products for glycerol esterification as determined with M06-2X/6-311+G(d,p) can be found in Table S1 Supplementary information.

Table 6 summarizes seven possible elementary steps for the acetylation of glycerol with acetic acid. Those thermodynamic quantities computed in Table 6 can also be considered as the relative stability of triacetin derivatives with respect to glycerol. The reaction free energy of an elementary step depends on the stability of reactants and products which in turn depends on their structures, i.e., position in which the reaction takes place, and the number and position of acetyl substituents.

It can be seen that the energetically favored path for the TAG formation is through 1-MAG because the acetylation of glycerol to produce 1-MAG is more exergonic than 2-MAG

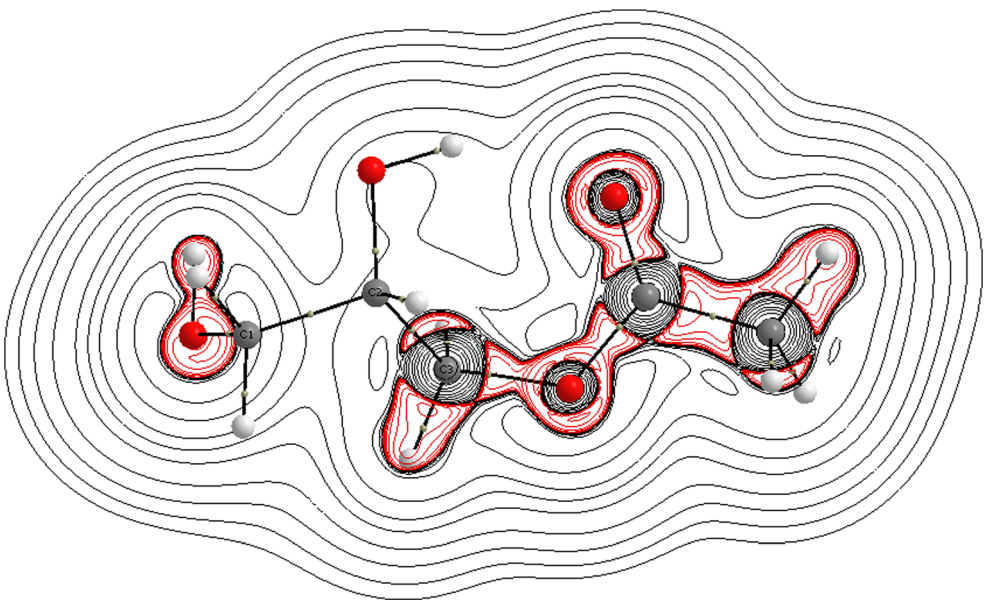

Fig. 3 Laplacian of the electronic charge density of 1-MAG in the plane that contains C-O-C bonded atoms of ester group. *Red* (broken) lines represent regions of electronic charge concentration and solid *black* lines denote regions of electronic charge depletion. Bond CP are indicated by *gray* circles. The molecular graph is also indicated. The contours of the Laplacian of the electronic charge density increase and decrease from a zero contour in steps of $\pm 2\times 10^n$, $\pm 4\times 10^n$, and $\pm 8\times 10^n$, with n beginning at −3 and increasing by unity

Scheme 2 Plausible reaction mechanism for the catalytic esterification of glycerol with acetic acid

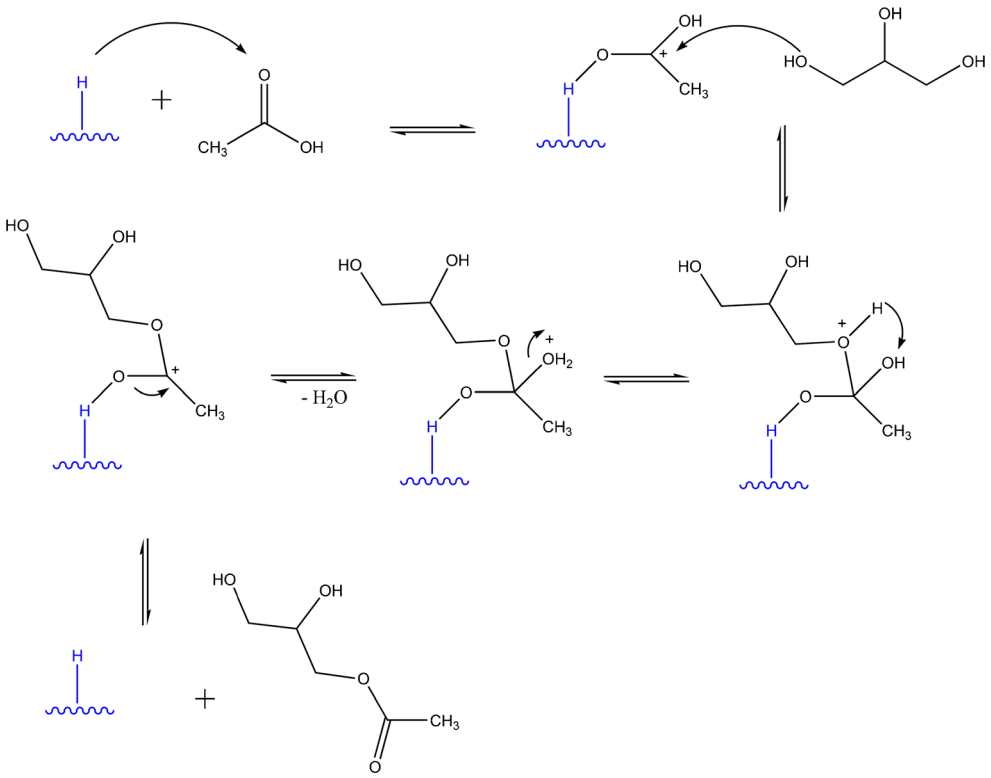

production. From a thermodynamics point of view, the esterification on primary carbon atom of glycerol is, therefore, more favorable than on secondary carbon atom. In other words, in solution phase the reaction follows these trends: G→1-MAG>G→2-MAG and side positions > middle position.

Then, as predicted by the NBCP values on oxygen atoms of the side and middle OH in the 1-MAG, the formed molecule, may further undergo acetylating on another external oxygen atom to generate the diacetylated derivatives. Judging from the reaction free energies, 1-MAG→1,3-DAG>1-MAG→1,2-DAG and this trend reflects that the nucleophile prefers to attack at the side position of 1-MAG.

Table 6 Reaction free energies[a,b] for seven elementary steps for glycerol acetylation

	Reaction	ΔG (kJ mol^{-1})
(1)	G + HAc = 1-MAG + W	−9.01
(2)	G + HAc = 2-MAG + W	−0.46
(3)	1-MAG + HAc = 1,2-DAG + W	−5.48
(4)	1-MAG + HAc = 1,3-DAG + W	−12.32
(5)	2-MAG + HAc = 1,2-DAG + W	−14.03
(6)	1,2-DAG + HAc = TAG + W	−11.82
(7)	1,3-DAG + HAc = TAG + W	−4.98

[a] Calculations at M06-2X/6-311+G(d,p) level). Solvent effects are included with the SCRF (PCM) method

[b] Reaction conditions: temperature = 413 K, pressure = 405.3 kPa

Finally, the diacetins may react with another molecule of acetic acid producing the triacetylated derivative. At this late state, 1,3-DAG structure is lower in energy than its possible competitor 1,2-DAG. A second mode of formation of TAG is provided by the 1,2-DAG acetylation. It turns out that this route is less favorable than the first route described, namely via 1,3-DAG.

These findings are supported by experimental results (Table 1) showing that 1-MAG formation is preferred over 2-MAG formation (concentration of 1-MAG is about 18 times the concentration of 2-MAG) and 1,3-DAG formation is preferred over 1,2-DAG formation (1,3-DAG concentration is twice the 1,2-DAG concentration).

According to the energies calculated at the M06-2X/6-311+G(d,p) level (Table 6) and taking into account the experimental results, it is possible to consider that glycerol is converted into triacetin through the thermodynamically favored pathway G→1-MAG→1,3-DAG→TAG via reactions

Table 7 Relative Gibbs energies (ΔG) and Boltzmann contribution at 413 K and 405.3 kPa for mono and diacetilated compounds[a]

Compound	ΔG (kJ mol^{-1})	Boltzmann contribution (%)[a]
1-MAG	0.00	96
2-MAG	8.55	4
1,2-DAG	6.84	29
1,3-DAG	0.00	71

[a] Calculated at 413 K and 405.3 kPa

(1), (4), and (7), meanwhile, the pathway through 2-MAG and 1,2-DAG is less energetically favored.

Theoretical prediction of the relationship between products

The corresponding Boltzmann contribution for several minimum energy isomers of MAG and DAG were evaluated and the relative proportion of the conformers was estimated. The contribution of each possible conformer was calculated according to the Eq. (1):

$$P_k = \exp\left(-\frac{\Delta G_k}{RT}\right) \Big/ \sum_i \exp\left(-\frac{\Delta G_i}{RT},\right) \quad (1)$$

where P_k represents the Boltzmann contribution for the conformer k.

The Gibbs free energy differences related to the most-stable conformer (ΔG) and the relative statistical weight of each conformer at 413 K are presented in Table 7.

Although there are three potential reaction sites in glycerol, only two isomers can be obtained by esterification: 1-MAG and 2-MAG. Assuming that the three sites are equally likely to undergo the esterification reaction, the contribution of 1-MAG to Maxwell-Boltzmann statistic should be twice. Thus, the calculated Boltzman distribution of 1-MAG to the reaction is 96 % while the contribution of 2-MAG is only 4 % at 413 K.

Similar conclusions can be drawn for DAG isomers. When one considers the overall reaction, it can be seen that 1-MAG can react giving both 1,2-DAG and 1,3-DAG, while 2-MAG can only react giving 1,2-DAG. The assumption of the same probability for each isomer is again adopted and so the relationship 3:1 for 1,2-DAG:1,3-DAG is used. This point is particularly important because it implies that the Boltzmann contribution is 29 % for 1,2-DAG and 71 % for 3-DAG.

From Table 1 values, the normalized results for monoacetins are 95 % (1-MAG) and 5 % (2-MAG). In a similar sense, the normalized results for diacetins are 33 % (1,2-DAG) and 67 % (1,3-DAG). The calculated Boltzmann distribution at 413 K (Table 7) and the the one observed experimentally (Table 1) are remarkably similar.

Thus, it is concluded that a thermodynamic control of the overall esterification reaction of glycerol with acetic acid occurs and G→1-MAG→1,3-DAG→TAG is the appropiate path for the reaction.

Conclusions

In this paper, the esterification reaction of glycerol with acetic acid has been studied both experimentally and theoretically. The experimental information was obtained at 413 K and 405.3 kPa, with molar relationship acetic acid:glycerol = 6:1 and Amberlyst 36 as catalyst. Theoretical calculations were performed at M06-2X/6-311+G(d,p) level including solvent effects through the polarizable continuum model.

Through the conformational analysis the most stable structures of the reactants and products were located from a large number of conformers. The lowest energy conformers found for the acetylated derivatives agree well with previously published results.

Topological charge density analysis performed at M06-2X/6-311++G(d,p) level showed that the properties evaluated at the BCP corresponds to interactions attributable to covalent or polarized bonds, in agreement with similar results.

NBCP calculated on oxygen atoms for glycerol and 1-monoacetin show that oxygen atoms of external OH have higher values of the NBCP than oxygen atoms of internal OH suggesting that external OH is easier to attack. Therefore the formation of 1-MAG could be favored over 2-MAG and the 1,3-DAG formation could be favored over the 1,2-DAG formation.

According to the energies calculated at the M06-2X/6-311+G(d,p) level, the thermodynamically favored reactions correspond to the pathway through 1-MAG and 1,3-DAG. Therefore, under the experimental reaction conditions employed here, i.e., 413 K and 405.3 kPa, the relative distribution of the products of esterification reaction is in excellent agreement with the findings in the theoretical calculations.

In summary, it is argued that a thermodynamic control of the overall esterification reaction of glycerol with acetic acid occurs and the esterification on the primary carbon atom is more favorable than on the secondary carbon atom. Therefore, the transformation of glycerol into 1-MAG and then into 1,3-DAG to produce TAG seems to be the appropriate path for the reaction.

Acknowledgments The authors acknowledge Consejo Nacional de Investigaciones Científicas y Técnicas (CONICET) and Universidad Nacional del Chaco Austral (UNCAUS) for financial support. NBO and CLP are members of the Scientific Research Career of CONICET. GAB is a fellowship of CONICET. The contribution of Dr. Reinaldo Pis Diez for extensive discussion on the subject and generous help in manuscript preparation is also gratefully acknowledged. Universidad Nacional de Catamarca (UNCA) is also appreciated for their computation supports.

References

1. Ma F, Hanna MA (1999) Biodiesel production: a review. Bioresour Technol 70:1–15
2. Liao X, Zhu Y, Wang SG, Li Y (2009) Producing triacetylglycerol with glycerol by two steps: esterification and acetylation. Fuel Process Technol 90:988–993
3. Johnson DT, Taconi KA (2007) The glycerin glut: options for the value-added conversion of crude glycerol resulting from biodiesel production. Environ Prog 26:338–348

4. Klepácová K, Mravec D, Kaszonyi A, Bajus M (2007) Etherification of glycerol and ethylene glycol by isobutylene. Appl Catal A 328:1–13
5. Klepácová K, Mravec D, Bajus M (2005) tert-Butylation of glycerol catalysed by ion-exchange resins. Appl Catal A 294:141–147
6. Noureddini H, Daily WR, Hunt BA (1998) Production of ethers of glycerol from crude glycerol-the by-product of biodiesel production. Chem Biomol Eng Res 13:121–129
7. Delfort B, Durand I, Jaecker A, Lacome T, Montagne X, Paille F (2005) Diesel fuel compounds containing glycerol acetals. Institut Francais du Petrole. US patent: US6890364
8. Delgado PJ (2009) Procedure to obtain biodiesel fuel with improved properties at low temperature. I.M.S.A, US patent: US7637969 B2
9. Melero JA, Vicente G, Morales G, Paniagua M, Bustamante J (2010) Oxygenated compounds derived from glycerol for biodiesel formulation: influence on EN 14214 quality parameters. Fuel 89:2011–2018
10. De Torres M, Jiménez-Osés G, Mayoral JA, Pires E, de los Santos M (2012) Glycerol ketals: synthesis and profits in biodiesel blends. Fuel 94:614–616
11. Rahmat N, Abdullah AZ, Mohamed AR (2010) Recent progress on innovative and potential technologies for glycerol transformation into fuel additives: a critical review. Renew Sust Energ Rev 14(3):987–1000
12. Nebel B, Mittelbach M, Uray G (2008) Determination of the composition of acetylglycerol mixtures by 1H NMR followed by GC investigation. Anal Chem 80:8712–8716
13. Lal SND, O'Connor CJ, Eyres L (2006) Application of emulsifiers/stabilizers in dairy products of high rheology. Adv Colloid Interf Sci 123–126:433–437
14. Behr A, Eilting J, Irawadi K, Leschinski J, Lindner F (2008) Improved utilisation of renewable resources: new important derivatives of glycerol. Green Chem 10:13–30
15. Zhou C-H, Beltramini JN, Fan Y-X, Lu GQ (2008) Chemoselective catalytic conversion of glycerol as a biorenewable source to valuable commodity chemicals. Chem Soc Rev 37:527–549
16. Guerrero-Perez MO, Rosas JM, Bedia J, Rodriguez-Mirasol J, Cordero T (2009) Recent inventions in glycerol transformations and processing, recent pat. Chem Eng 2:11–21
17. Troncea SB, Wuttke S, Kemnitz E, Coman SM, Parvulescu VI (2011) Hydroxylated magnesium fluorides as environmentally friendly catalysts for glycerol acetylation. Appl Catal B 107:260–267
18. Dosuna-Rodríguez I, Gaigneaux EM (2012) Glycerol acetylation catalysed by ion exchange resins. Catal Today 195:14–21
19. Izquierdo JF, Montiel M, Palés I, Outón PR, Galán M, Jutglar L, Villarrubia M, Izquierdo M, Hermo MP, Ariza X (2012) Fuel additives from glycerol etherification with light olefins: state of the art. Renew Sust Energ Rev 16:6717–6724
20. Gonçalves VLC, Pinto BP, Silva JC, Mota CJA (2008) Acetylation of glycerol catalyzed by different solid acids. Catal Today 133–135:673–677
21. Melero JA, van Grieken R, Morales G, Paniagua M (2007) Acidic mesoporous silica for the acetylation of glycerol: synthesis of bioadditives to petrol fuel. Energy Fuel 21:1782–1791
22. Díaz I, Márquez-Alvarez C, Mohino F, Pérez-Pariente J, Sastre E (2000) Combined alkyl and sulfonic acid functionalization of MCM-41-type silica. Part II. Esterification of glycerol with fatty acids. J Catal 193:295–302
23. Díaz I, Mohino F, Pérez-Pariente J, Sastre E (2003) Synthesis of MCM-41 materials functionalised with dialkylsilane groups and their catalytic activity in the esterification of glycerol with fatty acids. Appl Catal A 242:161–169
24. Diaz I, Mohino F, Blasco T, Sastre E, Pérez-Pariente J (2005) Influence of the alkyl chain length of HSO_3-R-MCM-41 on the esterification of glycerol with fatty acids. Microporous Mesoporous Mater 80:33–42
25. Ferreira P, Fonseca IM, Ramos AM, Vital J, Castanheiro JE (2009) Esterification of glycerol with acetic acid over dodecamolybdophosphoric acid encaged in USY zeolite. Catal Commun 10:481–484
26. Ferreira P, Fonseca IM, Ramos AM, Vital J, Castanheiro (2011) Acetylation of glycerol over heteropolyacids supported on activated carbon. Catal Commun 12:573–576
27. Ferreira P, Fonseca IM, Ramos AM, Vital J, Castanheiro JE (2009) Glycerol acetylation over dodecatungstophosphoric acid immobilized into a silica matrix as catalyst. Appl Catal B 91:416–422
28. Rezayatand M, Ghaziaskar HS (2009) Continuous synthesis of glycerol acetates in supercritical carbon dioxide using Amberlyst 15®. Green Chem 11:710–715
29. Zhou L, Nguyen T-H, Adesina AA (2012) The acetylation of glycerol over amberlyst-15: kinetic and product distribution. Fuel Process Technol 104:310–318
30. Zhou L, Al-Zaini E, Adesina AA (2013) Catalytic characteristics and parameters optimization of the glycerol acetylation over solid acid catalysts. Fuel 103:617–625
31. Liao X, Zhu Y, Wang S-G, Chen H, Li Y (2010) Theoretical elucidation of acetylating glycerol with acetic acid and acetic anhydride. Appl Catal B 94:64–70
32. Jamróz ME, Jarosz M, Witowska-Jarosz J, Bednarek E, Tęcza W, Jamróz MH, Dobrowolski JC, Kijeński J (2007) Mono-, di-, and tri-tert-butyl ethers of glycerol: a molecular spectroscopic study Original. Spectrochim Acta A 67:980–988
33. Bader RFW (1990) Atoms in molecules—a quantum theory. Clarendon, Oxford
34. Bader RFW, Popelier PLA, Keith TA (1994) Theoretical definition of a functional group and the molecular orbital paradigm. Angew Chem Int Ed Engl 33:620–631
35. Popelier P (2000) Atoms in molecules-an introduction. Prentice Hall, Harlow
36. Callam CS, Singer SJ, Lowary TL, Hadad CM (2001) Computational analysis of the potential energy surfaces of glycerol in the gas and aqueous phases: effects of level of theory, basis set, and solvation on strongly intramolecularly hydrogen-bonded systems. J Am Chem Soc 123:11743–11754
37. HyperChem (TM), Hypercube, Inc., Gainesville, FL
38. Dewar MJS, Zoebisch EG, Healy EF, Stewart JJP (1985) Development and use of quantum mechanical molecular models. 76. AM1: a new general purpose quantum mechanical molecular model. J Am Chem Soc 107:3902–3909
39. Berendsen HJC, Postma JPM, van Gunsteren WF, DiNola A, Haak JR (1984) Molecular dynamics with coupling to an external bath. J Chem Phys 81:3684–3690
40. Hohenberg P, Kohn W (1964) Inhomogeneous electron gas. Phys Rev 136:B864–B871
41. Kohn W, Sham LJ (1965) Self-consistent equations including exchange and correlation effects. Phys Rev 140:A1133–A1138
42. Parr R, Weitao Y (1994) Density-functional theory of atoms and molecules. Oxford University Press, New York
43. Frisch MJ et al. (2009) Gaussian 09, Revision A.1, Gaussian Inc., Wallingford, CT.
44. Becke AD (1993) Density-functional thermochemistry. III. The role of exact exchange. J Chem Phys 98:5648–5652
45. Lee C, Yang W, Parr RG (1988) Development of the Colle-Salvetti correlation energy formula into a functional of the electron density. Phys Rev B 37:785–789
46. Miehlich B, Savin A, Stoll H, Preuss H (1989) Results obtained with the correlation energy density functionals of becke and Lee, Yang and Parr. Chem Phys Lett 157:200–206
47. Zhao Y, Truhlar D (2008) The M06 suite of density functionals for main group thermochemistry, thermochemical kinetics, noncovalent interactions, excited states, and transition elements: two new functionals and systematic testing of four M06-class functionals and 12 other functionals. Theor Chem Accounts 120:215–241

48. Miertuš S, Scrocco E, Tomasi J (1981) Electrostatic interaction of a solute with a continuum. A direct utilization of AB initio molecular potentials for the prevision of solvent effects. Chem Phys 55:117–129
49. Miertus S, Tomasi J (1982) Approximate evaluations of the electrostatic free energy and internal energy changes in solution processes. Chem Phys 65:239–245
50. Tomasi J, Mennucci B, Cammi R (2005) Quantum mechanical continuum solvation models. Chem Rev 105:2999–3094
51. Keith TA. AIMAll (Version 13.02.26), in TK Gristmill Software. 2012: Overland Park KS (aim.tkgristmill.com)
52. Maccaferri G, Caminati W, Favero PG (1997) Free jet investigation of the rotational spectrum of glycerol. J Chem Soc Faraday Trans 93: 4115–4117
53. Champeney DC, Joarder RN, Dore JC (1986) Structural studies of liquid D-glycerol by neutron diffraction. Mol Phys 58:337–347
54. Garawi M, Dore JC, Champeney DC (1987) Structural studies of liquid D-glycerol II. Molecular conformation and long range correlations. Mol Phys 62:475–487
55. Koningsveld HV (1968) The crystal structure of glycerol and its conformation. Recl Trav Chem Pays-Bas 87:243–254
56. Limpanuparb T, Punyain K, Tantirungrotechai Y (2010) A DFT investigation of methanolysis and hydrolysis of triacetin. J Mol Struct THEOCHEM 955:23–32
57. Lilja J, Murzin D, Yu ST, Aumo J, Mäki-Arvela P, Sundell M (2002) Esterification of different acids over heterogeneous and homogeneous catalysts and correlation with the Taft Equation. J Mol Catal A 182–183:555–563
58. Kirumakki SR, Nagaraju N, Chary KVR (2006) Esterification of alcohols with acetic acid over zeolites Hβ, HY and HZSM5. Appl Catal A 299:185–192